Cholesterol Decreases the Interfacial Elasticity and Detergent Solubility of Sphingomyelins†

Xin-Min Li, Maureen M. Momsen, Janice M. Smaby, Howard L. Brockman, and Rhoderick E. Brown*

The Hormel Institute, University of Minnesota, 801 16th Avenue NE, Austin, Minnesota 55912

Received December 8, 2000; Revised Manuscript Received March 14, 2001

ABSTRACT: The interfacial interactions of cholesterol with sphingomyelins (SMs) containing various homogeneous acyl chains have been investigated by Langmuir film balance approaches. Low in-plane elasticity among the packed lipids was identified as an important physical feature of the cholesterol−sphingomyelin liquid-ordered phase that correlates with detergent resistance, a characteristic property of sphingolipid−sterol rafts. Changes in the in-plane elastic packing, produced by cholesterol, were quantitatively assessed by the surface compressional moduli (C_s^{-1}) of the monolayer isotherms. Of special interest were C_s^{-1} values determined at high surface pressures (>30 mN/m) that mimic the biomembrane situation. To identify structural features that uniquely affect the in-plane elasticity of the sphingomyelin−cholesterol lateral interaction, comparisons were made with phosphatidylcholine (PC)−cholesterol mixtures. Cholesterol markedly decreased the in-plane elasticity of either SM or PC regardless of whether they were fluid or gel phase without cholesterol. The magnitude of the reduction in in-plane elasticity induced by cholesterol was strongly influenced by acyl chain structure and by interfacial functional groups. Liquid-ordered phase formed at lower cholesterol mole fractions when SM's acyl chain was saturated rather than monounsaturated. At similar high cholesterol mole fractions, the in-plane elasticity within SM−cholesterol liquid-ordered phase was significantly lower than that of PC−cholesterol liquid-ordered phase, even when PCs were chain-matched to the SMs. Sphingoid-base functional groups (e.g., amide linkages), which facilitate or strengthen intermolecular hydrogen bonds, appear to be important for forming sphingomyelin−cholesterol, liquid-ordered phases with especially low in-plane elasticity. The combination of structural features that predominates in naturally occurring SMs permits very effective resistance to solubilization by Triton X-100.

The tendency of naturally occurring sphingolipids to mix nonrandomly with other lipids and form microdomains in model membranes has intrigued investigators for nearly two decades (*1*). More recent recognition that biomembranes may contain sphingolipid-sterol enriched microdomains or rafts with special functional roles has stimulated a great deal of interest. Among the proposed functions for these 'rafts' are trafficking and lateral distributional roles for certain signaling proteins and lipids in biomembranes (e.g., refs *2*−*5*).

Characterization of sphingolipid−cholesterol mixtures by various physical approaches has revealed a highly ordered and densely packed lipid environment when cholesterol mole fractions are sufficiently high (*1*, *6*). Hydrocarbon chain saturation is a key structural feature that enables cholesterol to form highly ordered and densely packed assemblies when mixed with simple sphingolipids (*7*−*9*). From these and other studies, a qualitative understanding has emerged regarding the lipid structural features that might favorably accommodate certain kinds of lipid anchors attached to proteins and enable resistance to solubilization by detergents (*8*, *10*−*12*).

It has been suggested that a key aspect of sphingolipid−cholesterol rafts is their liquid-ordered[1,2] (LO) phase character (*3*, *8*, *11*, *13*, *14*). Such phases are liquidlike with respect to the lateral diffusional capability of their component lipids but ordered in the sense that the acyl chains are extended and have fewer gauche rotamers due to their interactions with the planar ring of cholesterol (*15*−*17*). An important requirement for forming LO phase is cholesterol mole fractions in excess of about 0.25. Lower cholesterol mole

† We gratefully acknowledge the support of USPHS Grant GM45928 (to R.E.B.) and the Hormel Foundation. The automated Langmuir film balance used for this study received major support from USPHS Grant HL49180 (to H.L.B.). Portions of this investigation were presented in preliminary form at the FASEB Summer Conference on Molecular Biophysics of Cellular Membranes at Saxton's River, VT, July 1996; at the ASBMB Fall Symposium on Membrane Biogenesis at Lake Tahoe, CA, November 1998, and at the XIII Intl. Biophysics Congress Satellite Symposium on Membranes, Sensors, and Cell Surfaces at Hyderabad, India, September 1999.

* Correspondence should be addressed to this author: fax (507) 437-9606; phone (507) 433-8804; e-mail reb@tc.umn.edu.

[1] In the classic work of Ipsen et al. (*15*), the phase diagrams of cholesterol and DPPC were modeled within a two-dimensional lattice, and the terms liquid-ordered and liquid-disordered were defined and used for the first time. This model was not constrained to either bilayers or monolayers. Subsequent studies have shown many aspects of this model to be applicable to both bilayers and monolayers. Here, we also use the terms liquid-ordered and liquid-disordered and make no attempt to distinguish among various molecular descriptions of cholesterol-induced changes in phase structure (e.g., superlattices involving regular versus nonregular sterol distributions or dual upper miscibility critical points involving condensed complexes). For recent applications of the latter model to sphingomyelin−cholesterol mixtures, readers are referred to Radhakrishnan et al. (*33*, *63*). While this work was under review, Dietrich et al. (*71*) published an especially pertinent paper regarding the existence of sphingomyelin−cholesterol rafts in model membranes.

10.1021/bi002791n CCC: $20.00
Published on Web 04/26/2001

fractions promote a liquid-disordered phase structure with features consistent with liquid−liquid immiscibility (*18*−*20*). In arriving at the preceding picture, many studies have utilized dipalmitoylphosphatidylcholine (DPPC) to mimic sphingomyelin (SM) behavior (e.g., refs *12*, *13*, and *21*).

Like PC, SM has phosphocholine as its zwitterionic polar headgroup. Although SM and PC both have two long nonpolar hydrocarbon chains configured in rather similar ways, this is where the similarity ends. In PC, both hydrocarbon chains are ester-linked to a glycerol backbone, the *sn*-1 chain usually is saturated (e.g., palmitate or stearate), and the *sn*-2 chain usually contains one or more cis double bonds. In contrast, in SM, the sphingoid base serves the dual role as both interfacial backbone and nonpolar hydrocarbon chain. The only true acyl chain is amide-linked. Structural features that may impact on SM's ability to form specialized membrane environments include an abundance of long, saturated acyl chains that sometimes provide marked intramolecular chain-length asymmetry and interfacial functional groups that can donate and accept hydrogen bonds with neighboring lipids (*1*). While the latter feature has been the focus of many studies especially in relation to interactions with sterols (e.g., refs *16*, *22*, and *23*), the importance of acyl chain length and saturation has received much less attention despite indications that they may be pivotal to SM's mixing interactions with cholesterol (e.g., refs *7*, *8*, *10*, *11*, and *24*−*28*).

While the proposed LO nature of sphingolipid−sterol rafts provides a phenomenological framework for describing these microdomains (*1*, *6*, *4*), this lipid phase structure is not unique to mixtures of cholesterol and sphingomyelin or cholesterol and saturated-chain phosphoglycerides (e.g., DPPC/cholesterol). Similar phase diagrams have been reported for mixtures of cholesterol and PCs with saturated *sn*-1 and monounsaturated *sn*-2 acyl chains (*29*, *30*), although the critical sterol mole fraction appears to change with acyl composition (*31*−*34*). Issues that remain less clear are (i) the physical environment of the cholesterol−SM LO phase that set it apart from PC-based, LO phases; (ii) the structural features responsible for the SM-based LO phase being different; and (iii) the physical features of the SM-based LO phase that render it particularly suitable for biomembranes compared to other ordered phases (e.g., SM gel phase).

Here, we synthesized SMs with different homogeneous acyl chains, mixed them with cholesterol, and quantitatively assessed the changes in interfacial elasticity induced by cholesterol. Changes in in-plane elasticity are observed at cholesterol mole fractions likely to produce liquid-ordered phase behavior. Obtaining sufficiently low in-plane elasticities appears to be important for the lipid mixtures to resist solubilization by Triton X-100. Achieving low in-plane elasticity and Triton X-100 resistance in SMs or PCs depends on their hydrocarbon structure and configuration, their interfacial functional groups, and their cholesterol content.

MATERIALS AND METHODS

Egg and bovine brain SMs and all PCs were purchased from Avanti Polar Lipids (Alabaster, AL). Cholesterol was obtained from NuChek Prep (Elysian, MN). SMs containing homogeneous acyl chains were synthesized by reacylating sphingosylphosphocholine with the *N*-hydroxysuccinimide ester of the desired fatty acid (*35*, *36*). After purification by flash column chromatography and recrystallization, all lipids were greater than 99% pure on the basis of TLC analysis. Acyl homogeneity of the semisynthetic SM derivatives was confirmed by quantitatively releasing, methylating, and analyzing the fatty acyl residues via capillary gas chromatography as previously described (*35*). Egg SM acyl composition consisted of 86% palmitate (16:0), 0.4% myristate, 4.8% stearate (18:0), 1.1% arachidate (20:0), 2.5% behenate (22:0), 1.0% lignocerate (24:0), and 4.2% nervonate (24:$1^{\Delta 15}$). Bovine brain SM acyl composition consisted of 63% stearate (18:0), 2.4% palmitate (16:0), 6.6% arachidate (20:0), 9.2% behenate (22:0), 6.1% lignocerate (24:0), and 13% nervonate (24:$1^{\Delta 15}$). SMs and PCs were quantitated by phosphate assay (*37*), and cholesterol was quantitated gravimetrically.

Monolayer Conditions. SM stock solutions were prepared by dissolving lipids in either petroleum ether/ethanol (95:5), hexane/ethanol (95:5), or hexane/2-propanol/water (70:30:2.5). Solvent purity was checked by dipole potential measurements with a ^{210}Po ionizing electrode (*38*). Water for the subphase buffer was purified by reverse osmosis, activated charcoal adsorption, and mixed-bed deionization and then passed through a Milli-Q UV Plus System (Millipore Corp., Bedford, MA) and filtered through a 0.22 μm Millipak 40 membrane. Subphase buffer (pH 6.6) consisting of 10 mM potassium phosphate, 100 mM NaCl, and 0.2% NaN_3 was stored under argon until use. Glassware was acid-cleaned and rinsed thoroughly with deionized water and then with hexane/ethanol (95:5) prior to use.

Surface pressure−molecular area (π−A) isotherms were measured with a computer-controlled, Langmuir-type film balance, calibrated according to the equilibrium spreading pressures of known lipid standards (*39*). The standard errors of the isotherms are routinely less than 2%. Lipids were mixed and then spread (51.67 μL aliquots) from their dissolved stock solutions (see above). Films were compressed at a rate of $\leq$4 Å^2 molecule^{-1} min^{-1} after an initial delay period of 4 min. Previously, we showed that these conditions produced no hysteresis in the isotherms of various pure PCs (*41*). The subphase was maintained at fixed temperature in a thermostated, circulating water bath. The film balance was housed in an isolated laboratory supplied with clean air by a Bioclean Air Filtration system equipped with charcoal and HEPA filters. The trough was separately enclosed under humidified argon, cleaned by passage through a seven-stage series filtration setup consisting of an Alltech activated charcoal gas purifier, a LabClean filter, and a series of Balston disposable filters consisting of two adsorption (carbon) and three filter units (93% and 99.99% efficiency at 0.1 μm). Other technical features that contribute to isotherm reproducibility include automated lipid spreading

[2] Abbreviations: LO, liquid-ordered; SM, sphingomyelin; PC, diacyl-*sn*-glycero-3-phosphocholine; di-16:0 PC or DPPC, dipalmitoyl-*sn*-glycero-3- phosphocholine; 16:0 SM, *N*-16:0-sphingosylphosphocholine; 18:0 SM, *N*-18:0-sphingosylphosphocholine; 18:1 SM, *N*-18:$1^{\Delta 9(c)}$-sphingosylphosphocholine; BSM, bovine brain sphingomyelin; ESM, egg yolk sphingomyelin; 16:0,18:1 PC or POPC, 1-palmitoyl-2-oleoyl-*sn*-glycero-3-phosphocholine; di-14:0 PC or DMPC, dimyristoyl-*sn*-glycero-3-phosphocholine; 14:0,16:0 PC or MPPC, 1-myristoyl-2-palmitoyl-*sn*-glycero-3-phosphocholine; 14:0,18:0 PC or MSPC, 1-myristoyl-2-stearoyl -*sn*-glycero-3-phosphocholine; di-18:1 PC or DOPC, dioleoyl-*sn*-glycero-3- phosphocholine

via a modified HPLC autoinjector, automated surface cleaning by multiple barrier sweeps between runs, and highly accurate and reproducible setting of the subphase level by an automated aspirator.

Analysis of Isotherms. In keeping with recent proposals, we avoid using the term liquid-condensed and instead use the term condensed to denote monolayer states in which the hydrocarbon chains are ordered (*40*). The liquid-expanded state differs from the condensed state in that the chains are conformationally disordered. Monolayer phase transitions between the liquid-expanded and condensed states were identified from the second and third derivatives of surface pressure (π) with respect to molecular area (A) as previously described (*36, 41*).

Monolayer compressibilities at the indicated experimental mixing ratios were obtained from $\pi-A$ data by use of

$$C_s = (-1/A)(dA/d\pi) \quad (1)$$

where A is the area per molecule at the indicated surface pressure and π is the corresponding surface pressure (e.g., refs *42* and *43*). To facilitate comparison with elastic moduli of area compressibility values in bilayer systems (e.g., refs *44* and *45*), we expressed our data as the reciprocal of C_s, originally defined as the surface compressional modulus (C_s^{-1}) by Davies and Rideal (*42*). We used a 100-point sliding window that utilized every fourth point to calculate a C_s^{-1} value prior to advancing the window one point. Reducing the window size by as much as 5-fold did not significantly affect the C_s^{-1} values obtained. Each C_s^{-1} vs average molecular area curve consisted of 200 C_s^{-1} values obtained at equally spaced molecular areas along the $\pi-A$ isotherms. The standard error of the C_s^{-1} values is about 2%. High C_s^{-1} values correspond to low in-plane elasticity among packed lipids forming a monolayer. As shown in Smaby et al. (*53*), the C_s^{-1} values of PC−cholesterol mixtures are strongly affected by PC's acyl structure. When mixed with equivalent high cholesterol mole fractions, PCs with saturated acyl chains have much higher C_s^{-1} values than PCs with unsaturated acyl chains, suggesting that cis double bonds can act as interfacial springs that control the cholesterol-induced reduction in in-plane elasticity. For more comprehensive reviews of membrane micromechanical properties and of elasticity in two dimensions, readers are referred to Needham (*64*) and Behroozi *(43*). We found pure cholesterol monolayers, which are highly condensed, to have C_s^{-1} values of 1126, 1551, and 1540 mN/m at 10, 20, and 30 mN/m, respectively, in agreement with Merkel and Sackmann (*65*).

Assessment of Lipid Resistance to Detergent Solubilization by Light Scattering. Lipid solubilization by Triton X-100 was determined by light scattering as described by Xu and London (*12*). Multilamellar lipid vesicles (500 nmol lipid) were prepared by hydrating dried lipid films with buffer [10 mM HEPES (pH 6.6), 100 mM NaCl, and 0.02% NaN_3], briefly vortexing the hydrated lipid at temperatures 20−25 °C above their thermal phase transitions, and then cooling to room temperature for 4 h. As noted by Xu and London (*12*), we found the preceding approach to reduce variation associated with detergent solubilization data. Each lipid mixture was divided in half following preparation. One half served as control (no Triton X-100) and the remaining half was mixed with Triton X-100 to achieve a 15.5:1 molar ratio (detergent:lipid), which is similar to ratios used previously (*11, 12*). Controls and detergent-treated samples were incubated for 12 h at 24 °C prior to measurement of their optical densities at 400 nm (Beckman 600 spectrophotometer). Solubilization of lipid by detergent resulted in decreased light scattering and was expressed ratiometrically as the percent reduction in OD by dividing the OD of the sample mixed with Triton-X 100 by the OD of the detergentless control. Incubations carried out for up to 24 h showed that changes in OD occurred during the first 3 h following Triton X-100 addition. Other controls, in which light scattering was measured at 90° using a steady-state spectrofluorometer (*46*), yielded similar results.

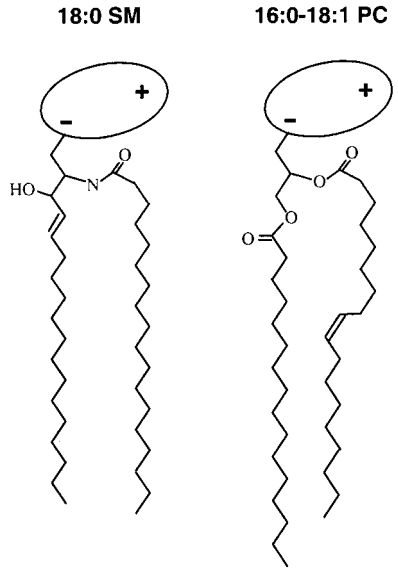

FIGURE 1: Structural features of naturally predominant sphingomyelin (SM) and phosphatidylcholine (PC). For simplicity, the lipid hydrocarbon chains are depicted as fully extended trans rotamers. In reality, free rotation about the carbon−carbon single bonds provides numerous trans−gauche isomers in the fluid but not the gel state. The cis double bond depicted in the *sn*-2 chain of PC leads to a t^+gt^- kink. Rotation about nearby carbon−carbon bonds increases the average molecular cross-sectional area. In PC, the glycerol base is depicted in gray and the highly hydratable, zwitterionic phosphocholine headgroup is depicted as a shaded ellipse oriented roughly parallel to the bilayer surface. In SM, the phosphocholine headgroup is depicted similarly, and a stearoyl (18:0) acyl chain, typical of bovine brain SM, is shown amide-linked to the 18-carbon sphingosine base, which contains a 4,5-trans double bond.

RESULTS

To evaluate SM structural features that might affect in-plane interactions with cholesterol and resulting solubilization by Triton X-100, the following was kept in mind regarding SM/PC structure (Figure 1). The first three carbons of the 18-carbon sphingoid base are configurationally similar to PC's glycerol backbone (*47*). Thus, PCs with ester-linked, saturated *sn*-1 acyl chains of about 14 carbons provide a close match with respect to hydrocarbon length. Also, the initial segment of the sphingosine base (carbons 1−5 including the 4,5-trans double bond) lies roughly orthogonal to the amide plane but with the hydroxyl on carbon 3 oriented toward the hydrated interface. The amide plane including the first two carbons of the N-linked acyl chain extends roughly parallel to the bilayer interface, but then the chain bends

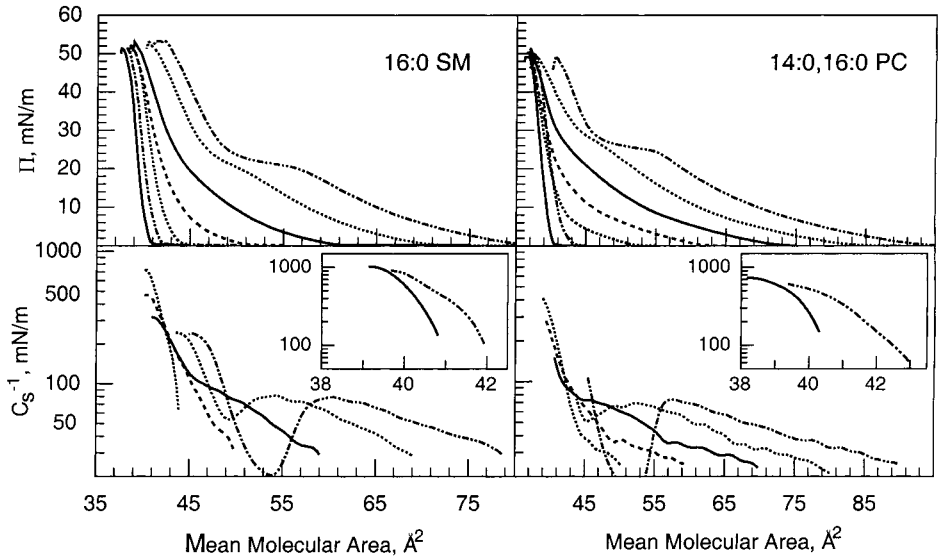

FIGURE 2: 16:0 SM/cholesterol (left panel) and 14:0,16:0 PC/cholesterol (right panel) mixed monolayers. Data were collected with an automated Langmuir-type film balance (see Materials and Methods). The standard errors are 2% or less. (Upper panel) Surface pressure versus average cross-sectional molecular area: isotherms (from right to left) contain 0 (− •• −), 0.1 (•••), 0.2 (—), 0.3 (---), 0.4 (•••), 0.5 (− •• −), and 0.6 (—) mole fraction sterol. (Lower panel) Surface compressional modulus (C_s^{-1}) versus average molecular area at 0 (− • • −), 0.1 (•••), 0.2 (—), 0.3 (---), and 0.4 (•••) mole fraction sterol. The insets show data for 0.5 (− •• −) and 0.6 (—) mole fraction cholesterol. The C_s^{-1}−A plots cover the surface pressure range of 1−30 mN/m. High C_s^{-1} values correspond to lipid packing arrangements with low in-plane elasticity.

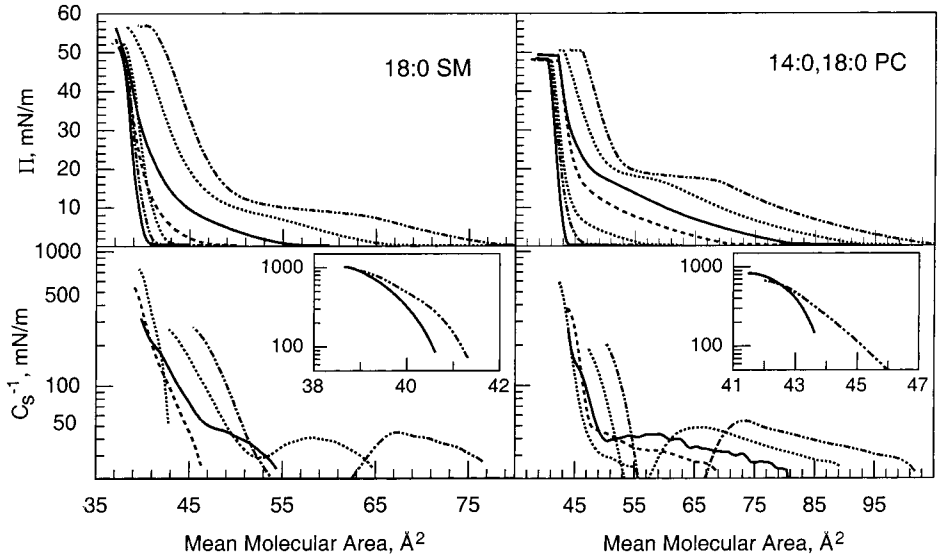

FIGURE 3: 18:0 SM/cholesterol (left panel) and 14:0,18:0 PC/cholesterol (right panel) mixed monolayers. (Other details are the same as in the caption for Figure 2.)

sharply to become parallel to the sphingoid base chain (*48*−*51*). The result is axial displacement of carbon atom positions along the two hydrocarbon chains, causing positional inequivalence. When the *N*-linked acyl chain contains a cis double bond, the positional axial displacement of carbon atoms will be exacerbated distal to the cis double bond due to the associated crank-shaft motif. Similar positional inequivalences exist along the ester-linked *sn*-2 chain of PC (*52*).

Cholesterol Reduces SMs In-Plane Elasticity More than That of Chain-Matched PCs. We and others have previously shown that mixing high cholesterol mole fractions with saturated PCs results in packing environments characterized by low in-plane elasticity in monolayers (*53*) and in bilayers (*44*, *54*). In contrast, the in-plane elasticity of PCs with unsaturated acyl chains is affected less by cholesterol (*45*, *53*). To determine how closely acyl-saturated PCs mimic the response of acyl-saturated SMs with respect to cholesterol-induced changes in in-plane elasticity, we measured the C_s^{-1} vs average molecular area behavior of 16:0 SM or 18:0 SM mixed with increasing cholesterol (Figures 2 and 3). We compared the results with those measured for cholesterol mixed with 14:0,16:0 PC or 14:0,18:0 PC, respectively, to minimize SM/PC hydrocarbon chain length differences. The upper panels of Figures 2 and 3 show the surface pressure versus average molecular area behavior at cholesterol mole fractions between 0 and 0.6. Two-dimensional phase transitions are evident in the isotherms of the SMs or PCs in the absence of sterol. The onset of these transitions occurs at slightly higher surface pressures for the PCs compared to the respective SMs. Cholesterol mole fractions above 0.2 eliminate the two-dimensional transitions. This is clearly

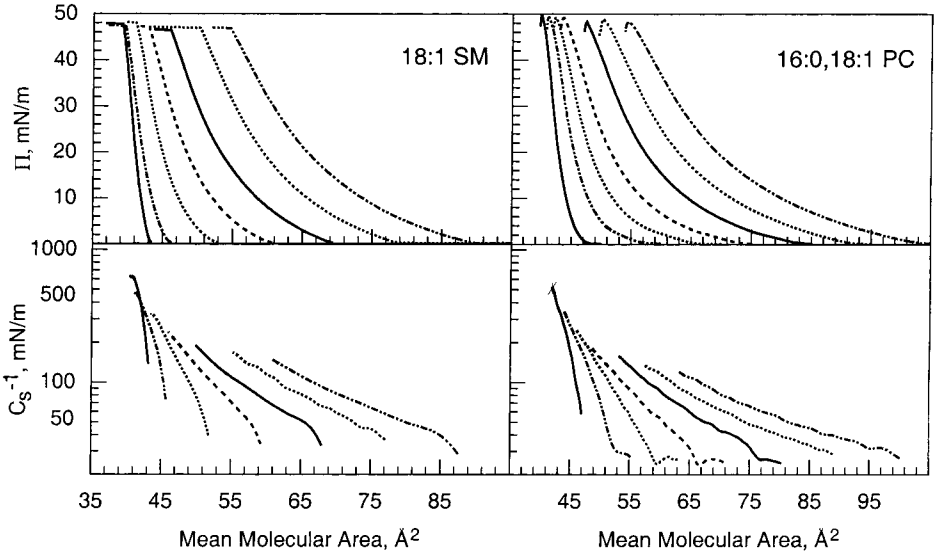

FIGURE 4: 18:1 SM/cholesterol (left panel) and 16:0,18:1 PC/cholesterol (right panel) mixed monolayers. Note that data shown in the right panels are consistent with those reported in Figure 3 of Smaby et al. (*53*). (Other details are the same as in the caption for Figure 2.)

evident in their C_s^{-1} vs average molecular area plots (Figures 2 and 3, lower panels), which show characteristic troughs in the two-phase coexistence region due to differences in the partial molar areas of the liquid-expanded (chain-disordered) and condensed (chain-ordered) phases (e.g., refs *36* and *41*). The disappearance of the liquid expanded-to-condensed transition is consistent with the general form of published phase diagrams in monolayers and bilayers (see introduction).

As cholesterol mole fractions increase above 0.2, C_s^{-1} values rise steadily. Figure 6 illustrates this response at various fixed surface pressures, where it is evident that cholesterol's impact is exacerbated at higher surface pressures. Moreover, at equivalent cholesterol mole fractions of 0.3 or higher, both 16:0 and 18:0 SM show 30−35% higher C_s^{-1} values than their chain-matched PC analogues (14:0,-16:0 PC and 14:0,18:0 PC, respectively). These differences are noteworthy because saturated-chain PCs have been used as sphingomyelin analogues in previous studies of raft lipids (e.g., refs *4*, *11*, and *13*). A comparison of the 30 mN/m C_s^{-1} values versus cholesterol mole fraction for several different PCs and SMs is summarized in Figure 8 (upper panels). The data obtained at 30 mN/m are of particular interest because high surface pressures (≥30 mN/m) mimic the biomembrane situation (*55*, *56*).

Acyl Unsaturation in SM Mitigates the Cholesterol-Induced Reduction in In-Plane Elasticity. If SM's amide and/or hydroxyl functional groups interact with cholesterol in ways that decrease in-plane elasticity beyond what can be attributed to chain conformation and acyl saturation, then modifications introduced somewhat distal to SM's interfacial functional groups should not be as disruptive to the interfacial elasticity as similar modifications in PC. To test this hypothesis, we compared the interfacial behavior of cholesterol mixed with either 18:1 SM or 1-palmitoyl-2-oleoyl-PC (16:0,18:1 PC). Figure 4 shows the resulting surface pressure (upper panels) and C_s^{-1} (lower panels) versus average molecular area for the mixtures. Both 18:1 SM and POPC exhibit chain-disordered, liquid-expanded behavior in the absence of cholesterol at all surface pressures below collapse. Mixing cholesterol with 18:1 SM or POPC at increasing mole fractions results in decreasing mean molecular areas. This behavior is not surprising given that pure cholesterol behaves as relatively small, component with a relatively fixed area (36−38 Å²/molecule) compared to pure 18:1 SM or POPC and that cholesterol also has a significant ordering effect, i.e., area condensing effect, on both 18:1 SM and POPC (*10*, *26*).

Increasing cholesterol content in 18:1 SM or POPC significantly increased the C_s^{-1} values but to a lesser extent than observed in SMs or PCs containing saturated acyl chains (Figures 4 and 7, lower panels). Yet the C_s^{-1} values of 18:1 SM at sterol mole fractions above 0.2 were higher than those observed for 16:0,18:1 PC at identical cholesterol content (Figure 7, lower panels). The observed differences in C_s^{-1} may explain the increased capacity for 18:1 SM to shield cholesterol from oxidation by cholesterol oxidase compared to PCs such as 18:0 and 18:1 PC as well as reported differences in sterol desorption from SM versus PC monolayers to β-cyclodextrin (*57*, *27*).

Cholesterol Reduces the In-Plane Elasticity of Naturally Occurring SMs. Egg SM and bovine brain SM are heterogeneous with respect to acyl composition. Egg SM is highly enriched in 16:0 SM (∼85%), with another 10% of other saturated species and 5% of monounsaturated species, whereas bovine brain SM is enriched in 18:0 SM (∼65%), with another 20% other long saturated species and 15% monounsaturated species (see Materials and Methods). The acyl heterogeneity including the presence of monounsaturated chains would be expected to impact cholesterol's ability to modulate in-plane elasticity. Figure 5 shows the effect of increasing cholesterol on the force−area and C_s^{-1}−area behaviors of egg SM and bovine brain SM. In the absence of sterol, both of these SMs display two-dimensional phase transitions, but the sharpness is reduced because of acyl chain heterogeneity (*35*). The C_s^{-1} values achieved upon mixing increasing cholesterol with egg or bovine brain SM are consistent with values expected for SMs with saturated acyl chains but are diminished somewhat, probably due to the presence of monounsaturated chains and the mix of different saturated acyl chains. This is especially evident for the more heterogeneous bovine brain SM (Figure 7, upper panels).

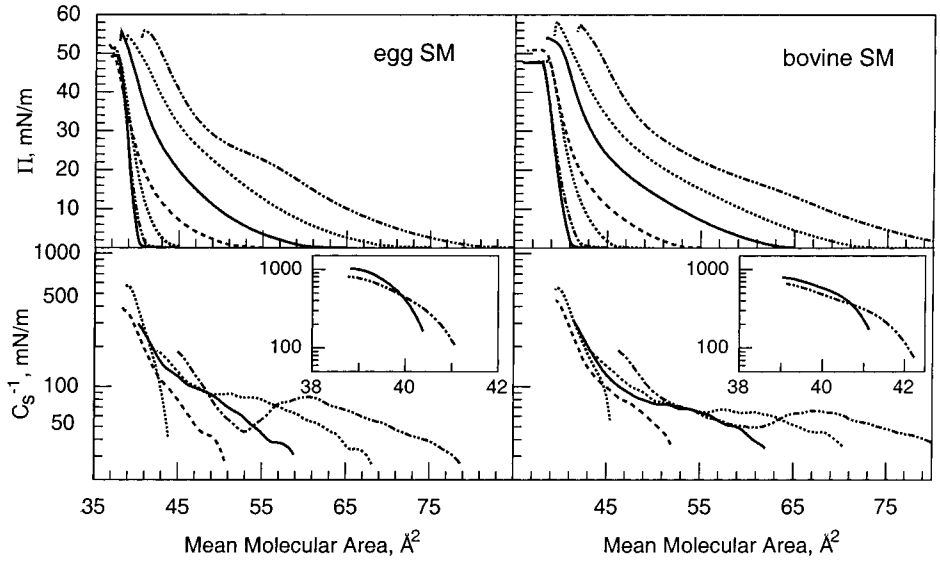

FIGURE 5: Egg SM/cholesterol (left panel) and bovine SM/cholesterol (right panel) mixed monolayers. (Other details are the same as in the caption for Figure 2.)

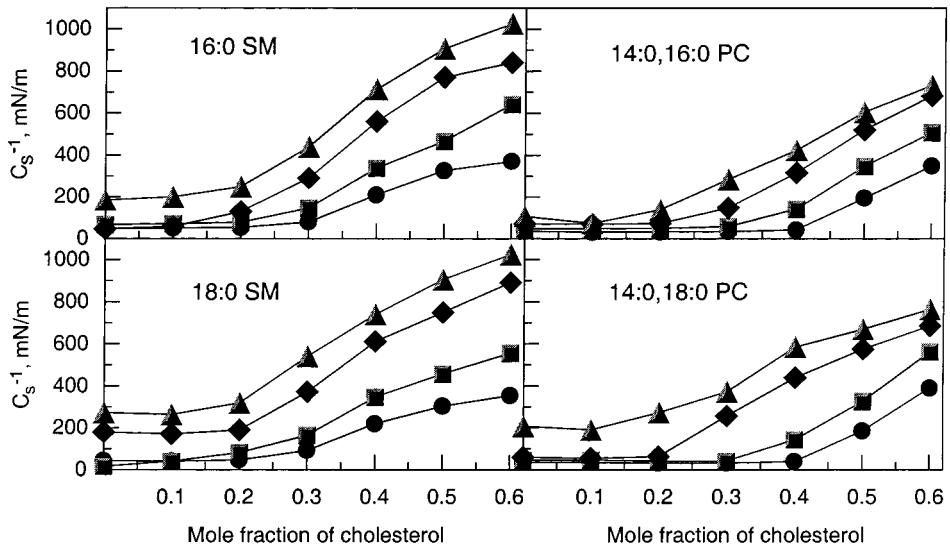

FIGURE 6: Surface compressional moduli (C_s^{-1}) versus sterol composition for 16:0 SM/cholesterol, 14:0,16:0 PC/cholesterol, 18:0 SM/cholesterol, and 14:0,18:0 PC mixed monolayers. The standard errors are 2% or less. Surface pressures are indicated by the following symbols: 5 mN/m (●), 10 mN/m (■), 20 mN/m (◆), and 30 mN/m (▲).

Cholesterol-Induced Liquid-Ordered Phase Has Lower In-Plane Elasticity than either Liquid-Expanded or Condensed Phase. Above 0.3 mole fraction, cholesterol dramatically reduces the in-plane elasticity of fluid-phase PCs but the extent of reduction depends on the number and location of cis double bonds in PC's acyl chains (*53*). At 30 mN/m, the largest cholesterol-induced changes in C_s^{-1} values of fluid-phase PCs occur when both acyl chains are saturated [e.g., fluid-phase DMPC = 110 mN/m; DMPC:chol (1:1) = 580 mN/m]. The results of the present study show that the C_s^{-1} values achieved in the chain-ordered, condensed phases of pure PCs or SMs are significantly lower than those attained upon mixing with high cholesterol. For instance, at 30 mN/m, the phase state of MSPC and 18:0 SM is condensed, i.e., chain-ordered, as is reflected by their respective cross-sectional areas (50 and 45 Å^2/molecule) and C_s^{-1} values (208 and 280 mN/m). When mixed with equimolar cholesterol, the mean cross-sectional areas of MSPC and 18:0 SM decrease to 42 and 39 Å^2/molecule, respectively, while their C_s^{-1} values increase to 670 and 906 mN/m (Figure 6). Under the same conditions, pure chain-ordered DPPC has a cross-sectional area of 46 Å^2/molecule and a C_s^{-1} value of 265 mN/m, whereas DPPC's equimolar cholesterol mix has a mean molecular area of 40 Å^2/molecule and a C_s^{-1} value of 706 mN/m (Figure 8, upper right panel). Thus, despite having highly ordered hydrocarbon chains, the in-plane elasticities of the LO and condensed phases differ significantly.

Detergent Resistance of SM−Cholesterol and Chain-Matched PC−Cholesterol Mixtures. If the in-plane elasticity of SM−cholesterol mixtures correlates with resistance to solubilization by Triton X-100, achieving sufficiently high C_s^{-1} values should limit or prevent Triton X-100 solubilization. To test this hypothesis, we used light scattering approaches to monitor Triton X-100 solubilization of select SM and PC derivatives in the absence and presence of increasing amounts of cholesterol as described by Xu and London (*12*). Figure 8 (lower panels) shows the percent change in optical density observed following incubation with

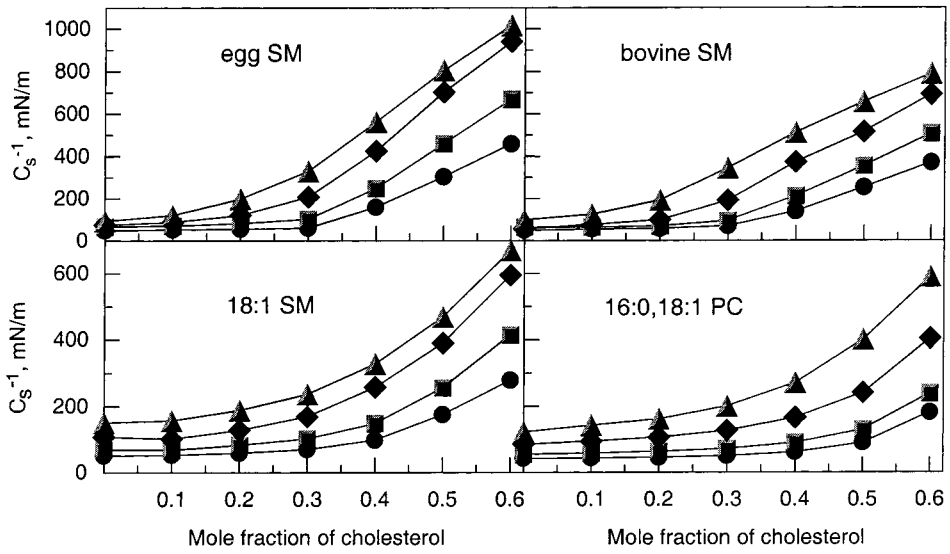

FIGURE 7: Surface compressional moduli (C_s^{-1}) versus sterol composition for egg SM/cholesterol, bovine SM/cholesterol, 18:1 SM/cholesterol, and 16:0,18:1 PC mixed monolayers. (Other details are the same as in the caption for Figure 6.)

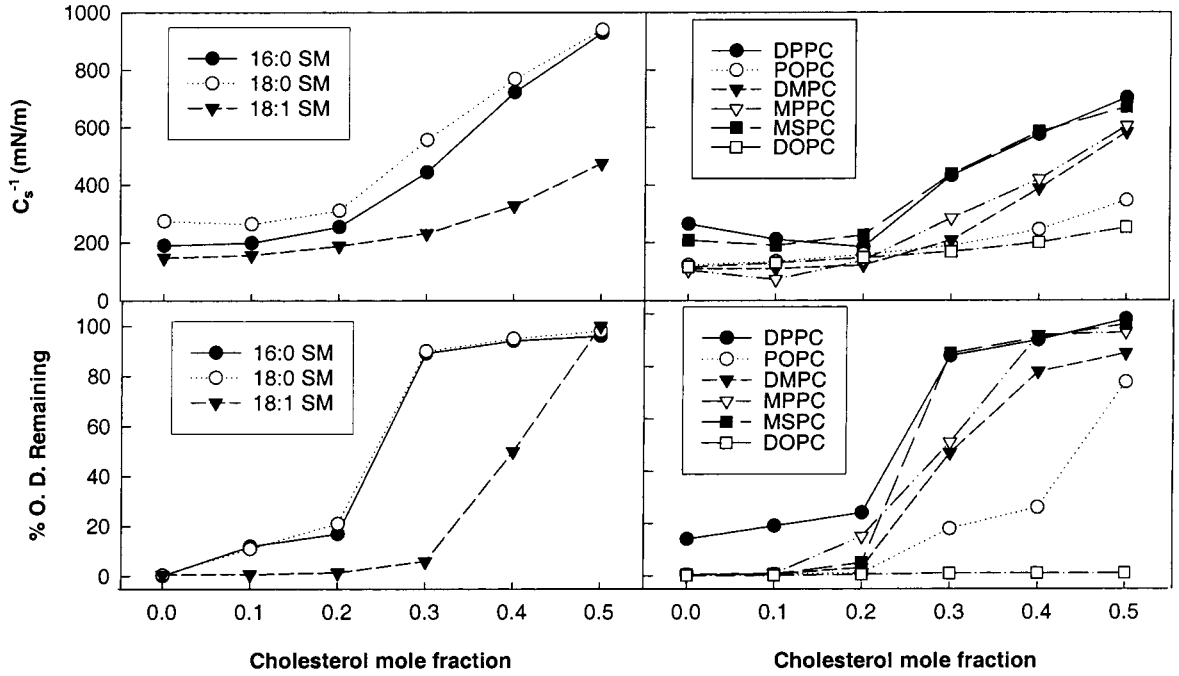

FIGURE 8: Comparison of monolayer surface compressional moduli (C_s^{-1}) and bilayer detergent insolubility of lipid mixtures of cholesterol and SM or PC. (Upper left panel) C_s^{-1} vs cholesterol mole fraction of SM/cholesterol mixtures at 30 mN/m and 24 °C. The standard errors are 2% or less. 16:0 SM (●); 18:0 SM (○); 18:1 SM (▼). Values at zero mole fraction cholesterol are consistent with those reported previously by Smaby et al. (*35*) and Li et al. (*36*). (Upper right panel) C_s^{-1} vs cholesterol mole fraction of PC/cholesterol mixtures at 30 mN/m and 24 °C. The standard errors are 2% or less. DPPC (●); POPC (○); DMPC (▼); MPPC (▽); MSPC (■); DOPC (□). Values reported for DMPC, POPC, and DOPC also appear in Smaby et al. (*53*). (Lower panels) Solubilization of lipid mixtures by Triton X-100 at 24 °C as determined by optical density change (% OD change). The standard errors are 5% or less. (Symbols are the same as for the upper panels).

Triton X-100 (see Materials and Methods). Equilibration times of 3 h showed no further change in optical density. Solubilization depended upon the mole fraction of cholesterol as well as the SM or PC acyl chain composition. For 16:0 SM, 18:0 SM, and PCs with saturated acyl chains (e.g., DPPC, DMPC, MPPC, and MSPC), dramatic increases in resistance to Triton X-100 solubilization at 24 °C were evident at cholesterol mole fractions between 0.2 and 0.3. Changing the acyl chain from 18:0 to 18:1 in SM increased the mole fraction of cholesterol necessary to achieve resistance to Triton X-100 solubilization (Figure 8). Similar behavior was observed in POPC−cholesterol mixtures except that even higher amounts of cholesterol were necessary. When both PC acyl chains were monounsaturated (18:1), sterol mole fractions up to 0.5 did not prevent solubilization by Triton X-100, in agreement with previous reports (e.g., refs *8* and *11*).

DISCUSSION

The results of this study provide insights into the in-plane elastic packing interactions of cholesterol and SMs. Increasing cholesterol content reduces sphingomyelin's in-plane

elasticity in a nonlinear fashion over the biologically relevant sterol mole fraction range of 0−0.6. Slight or no decrease in in-plane elasticity is observed at low cholesterol mole fractions, whereas marked changes occur at sterol mole fractions higher than 0.2−0.3. This abrupt reduction in in-plane elasticity is consistent with proximity to a critical point(s) in the phase diagram (*32, 33, 63*) and correlates with conversion to liquid-ordered behavior in the sphingomyelin matrix (*16*).

The abrupt decrease in the in-plane elasticity that occurs at cholesterol mole fractions between 0.2 and 0.3 is not unique to SMs but also occurs in PCs (*53, 58*). In PCs, the trend is observed whether the acyl chains are saturated or unsaturated. However, increasing unsaturation acts to buffer the abruptness and diminish the extent of the decrease induced by cholesterol. Thus, the sharpest and largest decreases in in-plane elasticity occur with SMs or PCs that have saturated acyl chains regardless of whether the lipids are in liquid-crystalline or gel phase in the absence of cholesterol.

A particularly compelling aspect of this study is the large difference observed in the in-plane elasticities of pure SM (or PC) condensed phases compared to their cholesterol-rich mixtures. Relative to the chain-disordered, liquid-expanded phase, the in-plane elasticity of the condensed phase is reduced 2−3-fold, while that of the liquid-ordered phase at equimolar cholesterol is reduced 5−7-fold. One possible explanation for this observation is the following. Cholesterol is likely to act as a phosphocholine headgroup spacer because the sterol polar headgroup is small compared to SM/PC's phosphocholine, while the sterol's nonpolar cross-sectional area (∼37 Å^2/molecule) is similar to that of ordered SM/PC with a saturated chain(s) (∼39 Å^2/molecule). At mole fractions of 0.3 or higher, cholesterol enhances phosphocholine headgroup mobility (ref *1* and references therein) and increases molecular translational mobility in the SM/PC matrix (*15, 16, 19*). Thus, ordered states such as LO phase can form relatively fast and with fewer packing defects compared to pure SM or PC gel phases, which have longer range order but, because of lower molecular translational mobility, generally have more packing defects, especially in the absence of very long equilibration times and/or reduced temperatures. The preceding explanation is supported by other recent data. Freed and colleagues (*14*) have shown that SM and DPPC gel phases have substantially greater rotational diffusion rates and order parameters than their equimolar mixtures with cholesterol near room temperature. Thus, while the time scales and temperatures associated with our monolayer experiments are likely to be insufficient for the pure SM or PC gel phase to achieve a true equilibrium, this same situation is likely for eukaryotic biomembranes under physiological conditions. Having high cholesterol provides biomembranes with the capability for rapidly achieving highly ordered membrane regions likely to be favored by certain proteins.

Our results emphasize that, although clearly important, saturation of SM's acyl chain is not the only structural feature contributing significantly to the low in-plane elasticities achieved by mixing SM with cholesterol. When chain-matched with respect to conformation and saturation, SMs (e.g., 18:0 SM or 16:0 SM) achieve almost 25% higher C_s^{-1} values than PCs (e.g., 14:0,16:0 PC or 14:0,18:0 PC, respectively) upon mixing with equimolar cholesterol. This implies that intermolecular interactions between SM's mostly saturated hydrocarbon chains and cholesterol's planar steroid ring only partially account for the low in-plane elasticity. An added contribution is likely to arise from intermolecular hydrogen bonding between cholesterol's 3-OH group and SM's amide group (*22*). The C−N bond of an amide has enhanced ionic character and diminished rotational capacity compared to the C−O bond of an ester (*59*). This difference may help stabilize interfacial hydrogen bonds between cholesterol and SM.

Cholesterol-Induced Changes in In-Plane Elasticities of Monolayers and Bilayers. Because lateral interactions among neighboring lipids affect many physical phenomena in membranes, it not surprising that bilayer and monolayer model membranes mimic one another with respect to several fundamentally important features. For instance, changes in lipid translational diffusion rates that accompany the phase transitions of pure PCs (*66*) and that accompany increasing cholesterol mole fractions in PC (*65, 67*) are similar in both monolayers and bilayers.

In earlier monolayer studies involving SMs and cholesterol [ref *10* and references therein], interactions among the lipids were evaluated primarily from changes in the average cross-sectional area, i.e., area condensation. Subsequent studies have revealed inherent caveats in relying solely on area condensations at lower surface pressures to assess the in-plane interaction affinity of cholesterol for different sphingolipids or PCs (*10, 53*). The caveats occur because acyl structure alters the surface pressure response of the area condensation in complex and nonuniform ways, making it risky to arbitrarily extrapolate to the high surface pressure, biomembranelike situation (*53*). Moreover, accurately quantitating small changes in absolute lipid area at the high surface pressures that better mimic biomembrane conditions is beyond the practical capabilities of most instrumental systems. In contrast, C_s^{-1} measurements rely primarily on information contained within the shapes of the isotherms and are much less affected by the absolute area values. As a result, they provide a sensitive way to gain quantitative insights into the packing elasticity achieved over a range of surface pressures and cholesterol mole fractions, including those most relevant to biomembrane conditions. It is worth noting that the cholesterol-induced changes in bilayer and monolayer in-plane elasticities for various fluid-phase PCs are similar when the monolayer measurements are performed in the 30−35 mN/m surface pressure range (*45*−*53*).

Comparing SM monolayer and bilayer in-plane elasticity values is currently possible only for equimolar bovine SM and cholesterol. No bilayer data have appeared for pure SMs, presumably because of the technical challenges associated with manipulating pure gel-phase SM vesicles by micropipet aspiration. Yet, from work with bilayers, it is clear that chain saturation in SMs plays a major role in producing low-elasticity packing interactions with cholesterol (*45, 54*).

Low In-Plane Elasticity and Detergent Resistance. The trend of little change in in-plane elasticity until critical cholesterol mole fractions are reached, followed by rapidly increasing C_s^{-1} values at higher cholesterol mole fractions, is a response that is mirrored in the solubilization response of Triton X-100. When C_s^{-1} values are relatively low (<350 mN/m), SMs and PCs are largely solubilized by Triton X-100 at 24 °C (Figure 8). When sufficient cholesterol is present

for C_s^{-1} values to exceed ~400 mN/m, much less Triton X-100 induced solubilization is achieved.

With SMs or PCs containing saturated acyl chains, the relatively abrupt increases in resistance to Triton X-100 solubilization appear to approximate conversion to LO phase behavior. Schroeder et al. (*13*) observed similar behavior with DPPC−cholesterol mixtures. It is also clear that relying on Triton X-100 solubilization only approximates the amounts of LO phase domains (*21*). Assuming that resistance to solubilization by Triton X-100 does approximate conversion to LO behavior, then our results suggest that SM and PC with a single monounsaturated acyl chain (e.g., 18:1 SM or POPC) need higher amounts of cholesterol to achieve LO than their saturated counterparts. Indeed, Mateo et al. (*30*) investigated the POPC−cholesterol phase diagram and found cholesterol mole fractions of 0.4 or higher are required to form LO phase compared to cholesterol mole fractions of 0.3 in DMPC. Epifluorescence microscopy studies also suggest the need for higher cholesterol mole fractions to achieve LO phase in POPC−cholesterol monolayers (*68*). Our detergent resistance data appear to support these data. Conversion of 18:1 SM−cholesterol mixtures to LO has not been previously reported, although our detergent resistance data would suggest between 0.3 and 0.4 mole fraction is needed. With a PC in which both acyl chains are monounsaturated (DOPC), cholesterol mole fractions up to 0.5 fail to produce LO phase as judged by the modest increases in C_s^{-1} values and by the lack of resistance to Triton X-100 solubilization. The facile solubilization of DOPC−cholesterol mixtures by Triton X-100 is well established (*4*, *21*).

Implications. By studying the in-plane interactions of different sphingomyelin species and cholesterol, we have determined that the especially low in-plane elasticity of cholesterol−SM LO phase sets it apart from PC-based, LO phases. Moreover, the structural basis for SM-based LO phase being different is not simply due to the preponderance of saturated chains in naturally occurring SMs but also may involve the enhanced stability of hydrogen bonds involving amide linkages. Simple sphingolipids possess interfacial functional groups (e.g., amino and carbonyl groups of amide linkages, as well as hydroxyl groups) that can donate and accept intramolecular hydrogen bonds, whereas only hydrogen-bond acceptors (carbonyl groups of ester linkages) are present in PC's interfacial region. Importantly, however, the low in-plane elasticities needed to avoid Triton X-100 solubilization are most easily attained at physiological cholesterol concentrations when acyl chains are saturated. When SM's acyl chain is unsaturated, higher cholesterol mole fractions are required to achieve sufficiently low in-plane elasticity to avoid Triton X-100 solubilization. In this regard, naturally occurring SMs are particularly suited for achieving a liquid-ordered state of low in-plane elasticity at cholesterol contents within the physiological realm of many biomembranes. The low in-plane elasticities within SM−cholesterol liquid-ordered phases also distinguish them from other SM ordered phases such as pure gel phase and help explain observed differences in the Triton X-100 solubilization of these two types of phases. Thus, the physiologically relevant ordered phase in biomembranes is likely to be the cholesterol-induced liquid-ordered phase.

In biomembranes, the question of whether sphingolipid−cholesterol rafts really exist remains unsettled. One recent study suggests that sphingolipid−cholesterol rafts in the plasma membrane of fibroblast-like cells can diffuse as rather stable platforms with average areas of about 2100 nm^2 (*60*). Yet other compelling investigations raise serious concerns about raft existence based on their ability to cluster GPI-anchored proteins in plasma membranes (*61*). Our measurements of the in-plane packing elasticity of cholesterol mixed with various SM and PC species suggest that naturally abundant SMs are especially well suited for forming sterol-enriched microdomains in model membranes. Moreover, as pointed out previously (*69*), SM involvement in rafts makes the situation more intriguing because SMs are one of the few naturally occurring membrane lipids whose fluid−gel coexistence region is poised close to mammalian physiological temperatures. Cholesterol could easily modulate domain formation and size. While the inherent miscibility of the lipids can provide a favorable driving force for raft formation in model membranes, the problem in cell membranes appears to be controlling the size, location, and stability of such domains because plasma membranes contain relatively large amounts of SM and cholesterol. This has led to the idea that compartmentalization of rafts may occur via the membrane-associated cytoskeleton (*70*). In addition, specialized membrane proteins may play a role in altering the inherent miscibility of raft lipids. Interestingly, there is precedent for nonenzymic proteins laterally reorganizing the lipid composition of liquidlike interfaces to enhance lipolytic processes (*62*). Whether analogous lipid recruiting or segregating proteins play a role in controlling sphingolipid−sterol raft formation and size will require further study.

ACKNOWLEDGMENT

We thank Bonnie Hummel for helping to synthesize and purify certain of the SM derivatives.

REFERENCES

1. Brown, R. E. (1998) *J. Cell Sci. 111*, 1−9.
2. Simons, K., and Ikonen, E. (1997) *Nature 387*, 569−572.
3. Brown, D. A., and London, E. (1998) *Annu. Rev. Cell Dev. Biol. 14*, 111−136.
4. Brown, D. A., and London, E. (2000) *J. Biol. Chem. 275*, 17221−17224.
5. Simons, K., and Toomre, D. (2000) *Nat. Rev. Mol. Cell Biol. 1*, 31−39.
6. Rietveld, A., and Simons, K. (1998) *Biochim. Biophys. Acta 1376*, 467−479.
7. Silvius, J. R. (1992) *Biochemistry 31*, 3398−3408.
8. Schroeder, R., London, E., and Brown, D. A. (1994) *Proc. Natl. Acad. Sci. U.S.A. 91*, 12130−12134.
9. Ali, S., Smaby, J. M., Brockman, H. L., and Brown, R. E. (1994) *Biochemistry 33*, 2900−2906.
10. Smaby, J. M., Momsen, M., Kulkarni, V. S., and Brown, R. E. (1996) *Biochemistry 35*, 5696−5704.
11. Ahmed, S. N., Brown, D. A., and London, E. (1997) *Biochemistry 36*, 10944−10953.
12. Xu, X., and London, E. (2000) *Biochemistry 39*, 843−849.
13. Schroeder, R., Ahmed, S. N., Zhu, Y., London, E., and Brown, D. A. (1998) *J. Biol. Chem. 273*, 1150−1157.
14. Ge, M., Field, K. A., Aneja, R., Holowka, D., Baird, B., and Freed, J. H. (1999) *Biophys. J. 77*, 925−933.
15. Ipsen, J. H., Karlström, G., Mouritsen, O. G., Wennerström, H., and Zuckermann, M. J. (1987) *Biochim. Biophys. Acta 905*, 162−172.
16. Sankaram, M. B., and Thompson, T. E. (1990) *Biochemistry 29*, 10670−10675.

17. McMullen, T. P. W., and McElhaney, R. N. (1996) *Curr. Opin. Colloid Interface Sci. 1*, 83−90.
18. Subramaniam, S., and McConnell, H. M. (1987) *J. Phys. Chem. 91*, 1715−1718.
19. Vist, M. R., and Davis, J. H. (1990) *Biochemistry 29*, 451−464.
20. Zuckermann, M. J., Ipsen, J. H., and Mouritsen, O. G. (1993) in *Cholesterol in Membrane Models* (Finegold, L., Ed.) pp 223−257, CRC Press, Boca Raton, FL.
21. London, E., and Brown, D. A. (2000) *Biochim. Biophys. Acta 1508*, 182−195.
22. Bittman, R., Kasireddy, C. R., Mattjus, P., and Slotte, J. P. (1994) *Biochemistry 33*, 11776−11781.
23. Slotte, J. P. (1995) *Biochim. Biophys. Acta 1235*, 419−427.
24. Snyder B., and Freire, E. (1980) *Proc. Natl. Acad. Sci. U.S.A. 77*, 4055−4059.
25. Silvius, J. R., del Guidice, D., and Lafleur, M. (1996) *Biochemistry 35*, 15198−15208.
26. Smaby, J. M., Brockman, H. L., and Brown, R. E. (1994) *Biochemistry 33*, 9135−9142.
27. Ramstedt, B., and Slotte, J. P. (1999) *Biophys. J. 76*, 908−915.
28. Wang, T.-Y., and Silvius, J. R. (2000) *Biophys. J. 79*, 1478−1489.
29. Thewalt, J. L., and Bloom, M. (1992) *Biophys. J. 63*, 1176−1181.
30. Mateo, C. R., Acuña, A. U., and Brochon, J.-C. (1995) *Biophys. J. 68*, 978−987.
31. Hagan, J. P., and McConnell, H. M. (1997) *Biochim. Biophys. Acta 1329*, 7−11.
32. Radhakrishnan, A., and McConnell, H. M. (1999) *Biophys. J. 77*, 1507−1517.
33. Radhakrishnan, A., Anderson, T. G., and McConnell, H. M. (2000) *Proc. Natl. Acad. Sci. U.S.A. 97*, 12422−12427.
34. Keller, S. L., Radhakrishnan, A., and McConnell, H. M. (2000) *J. Phys. Chem. B 104*, 7522−7527.
35. Smaby, J. M., Kulkarni, V. S., Momsen, M., and Brown, R. E. (1996) *Biophys. J. 70*, 868−877.
36. Li, X.-M., Smaby, J. M., Momsen, M. M., Brockman, H. L., and Brown, R. E. (2000) *Biophys. J. 78*, 1921−1931.
37. Bartlett, G. R. (1959) *J. Biol. Chem. 234*, 466−468.
38. Smaby, J. M., and Brockman, H. L. (1991) *Chem. Phys. Lipids 58*, 249−252.
39. Momsen, W. E., Smaby, J. M., and Brockman, H. L. (1990) *J. Colloid Interface Sci. 135*, 547−552.
40. Kaganer, V. M., Möhwald, H., and Dutta, P. (1999) *Rev. Mod. Phys. 71*, 779−819.
41. Ali, S., Smaby, J. M., Momsen, M. M., Brockman, H. L., and Brown, R. E. (1998) *Biophys. J. 74*, 338−348.
42. Davies, J. T., and Rideal, E. K. (1963) *Interfacial Phenomena* (2nd Ed.), p 265, Academic Press, New York.
43. Behroozi, F. (1996) *Langmuir 12*, 2289−2291.
44. Evans, E., and Needham, D. (1987) *J. Phys. Chem. 91*, 4219−4228.
45. Needham, D., and Nunn, R. S. (1990) *Biophys. J. 58*, 997−1009.
46. Mattjus, P., Molotkovsky, J. G., Smaby, J. M., and Brown, R. E. (1999) *Anal. Biochem. 268*, 297−304.
47. Pascher, I., Lundmark, M., Nyholm, P.-G., and Sundell, S. (1992) *Biochim. Biophys. Acta 1113*, 339−373.
48. Speyer, J. B., Weber, R. T., Das Gupta, S. K., and Griffin, R. G. (1989) *Biochemistry 28*, 9569−9574.
49. Hamilton, K. S., Jarrell, H. C., Briere, K. M., and Grant, C. W. M. (1993) *Biochemistry 32*, 4022−4028.
50. Morrow, M. R., Singh, D., and Grant, C. W. M. (1995) *Biochim. Biophys. Acta 1235*, 239−248.
51. Ruocco, M. J., Siminovitch, D. J., Long, J. R., Das Gupta, S. K., and Griffin, R. G. (1996) *Biophys. J. 71*, 1776−1788.
52. Pearson, R. H., and Pascher, I. (1979) *Nature 281*, 499−501.
53. Smaby, J. M., Momsen, M., Brockman, H. L., and Brown, R. E. (1997) *Biophys. J. 73*, 1492−1505.
54. McIntosh, T. J., Simon, S. A., Needham, D., and Huang, C. (1992) *Biochemistry 31*, 2012−2020.
55. Marsh, D. (1996) *Biochim. Biophys. Acta 1286*, 183−223.
56. MacDonald, R. C. (1996) in *Vesicles* (Rosoff, M., Ed.) pp 3−48, Marcel Dekker, New York.
57. Mattjus, P., and Slotte, J. P. (1994) *Chem. Phys. Lipids 71*, 73−81.
58. Hirshfeld, C. L., and Seul, M. (1990) *J. Phys. (Paris) 51*, 1537−1552.
59. Wiberg, K. B., and Laidig, K. E. (1987) *J. Am. Chem. Soc. 109*, 5935−5943.
60. Pralle, A., Keller, P., Florin, E. L., Simons, K., and Horber, J. K. H. (2000) *J. Cell Biol. 148*, 997−1007.
61. Kenworthy, A. K., Petranova, N., and Edidin, M. (2000) *Mol. Biol. Cell 11*, 1645−1655.
62. Momsen, W. E., Momsen, M. M., and Brockman, H. L. (1995) *Biochemistry 34*, 7271−7281.
63. Radhakrishnan, A., Li, X.-M., Brown, R. E., and McConnell, H. M. (2001) *Biochim. Biophys. Acta 1511*, 1−6.
64. Needham, D. (1995) in *Permeability and Stability of Lipid Bilayers* (Dislavo, E. A., and Simon, S. A., Eds.) pp 49−76, CRC Press, Boca Raton, FL.
65. Merkel, R., and Sackmann, E. (1994) *J. Phys. Chem. 98*, 4428−4442.
66. Peters, R., and Beck, K. (1983) *Proc. Natl. Acad. Sci. U.S.A. 80*, 7183−7187.
67. Tanaka, K. Manning, P. A., Lau, V. K., and Yu, H. (1999) *Langmuir 15*, 600−606.
68. Worthman, L.-A. D., Nag, K., Davis, P. J., and Keough, K. M. W. (1997) *Biophys. J. 72*, 2569−2580.
69. Smaby, J. M., Momsen, M., Kulkarni, V. S., and Brown, R. E. (1996) *Biochemistry 35*, 5696−5704.
70. Jacobson, K. and Dietrich, C. (1999) *Trends Cell Biol. 9*, 534−542.
71. Dietrich, C., Bagatolli, L. A., Volovyk, Z. N., Thompson, N. L., Levi, M., Jacobson, K., and Gratton, E. (2001) *Biophys. J. 80*, 1417−1428.

BI002791N